Chinese Journal of Chemistry, **2004**, *22*, 590—593 **Article**

Mechanism and Kinetics for the Reaction of NCS and OH Radicals

LIU, Peng-Jun[a,b](刘朋军) ZHAO, Min[a](赵岷) CHANG, Ying-Fei[a](常鹰飞)
ZHAO, Yan-Ling[a](赵艳玲) SU, Zhong-Min[a](苏忠民) WANG, Rong-Shun*[,a](王荣顺)

[a] *Institute of Functional Material Chemistry, Faculty of Chemistry, Northeast Normal University, Changchun, Jilin 130024, China*
[b] *Department of Chemistry, Hainan Normal University, Haikou, Hainan 571158, China*

The mechanism and dynamical properties for the reaction of NCS and OH radicals have been investigated theoretically. The minimum energy paths (MEP) of the reaction were calculated using the density functional theory (DFT) at the B3LYP/6-311＋G** level, and the energies along the MEP were further refined at the QCISD(T)/6-311＋G** level. As a result, the reaction mechanism of the title reaction involves three channels, producing HCS＋NO and HNC＋SO products, respectively. Path I and path II are competitive, with some advantages for path I in kinetics. As for path III, it looks difficult to react for its high energy barrier. Moreover, the rate constant have been calculated over the temperature range of 800—2500 K using canonical variational transition-state theory (CVT). It was found that the rate constants for both path I and path II are negatively dependent on temperature, which is similar with the experimental results for reactions of NCS with NO and NO_2, and the variational effect for the rate constant calculation plays an important role in whole temperature range.

Keywords NCS radical, reaction mechanism, density functional theory (DFT), variational transition-state

Introduction

The reaction properties and kinetics of the nitrogen-containing radicals in the gas phase are very interesting, partly because these species play an important role in the formation and removal of NO_x pollutants in combustion chemistry.[1] For example, NCO is the most important intermediate in the RAPRENO$_x$ process.[2,3] Kinetic studies on the reactions of NCO with numerous species, including NO,[4-8] NO_2,[6,9] H_2,[4] CH_x,[10,11] and OH[12] have been reported. As we know the NCS radical is the isoelectronic species of NCO, and its spectrum is complicated due to the presence of Renner-Teller and spin orbit interactions.[13,14] The NCS radical which can join the RAPRENO$_x$ process is an intermediate in the combustion of sulfur-containing fuels. The kinetics of this radical with NO, NO_2, O_2 have been reported.[15] However, it is quite surprising that there are no reports of theoretical research on NCS radical. The objectives of the present study are to obtain the mechanism and dynamical properties theoretically for the reaction of NCS radical with OH.

Computational methods

All *ab initio* calculations were carried out using the GAUSSIAN98 program.[16] The optimized geometries and harmonic vibrational frequencies of the reactant, products, intermediates and transition states were obtained using the density functional theory (DFT) B3LYP method with 6-311＋G** basis set. The harmonic vibrational frequencies were used for the characterization of stationary points. All stationary points were positively identified for minimum (number of imaginary frequencies N＝0) or transition state (N＝1). The intrinsic reaction coordinate (IRC) calculations at the same level were also carried out to check the connection between all the critical structures located on the potential energy surface. Single-point calculations were further performed at the QCISD(T)/6-311＋G** level using the B3LYP/6-311＋G** optimized geometries. The zero-point vibration energy (ZPVE) at the B3LYP/6-311＋G** level was also included. Unless otherwise specified, the QCISD(T)/6-311＋G** single-point energies were used in the following discussion. By means of the Polyrate 9.0 program,[17] the theoretical rate constants for both path I and path II over the temperature range of 800—2500 K were calculated using CVT theory.

Results and discussion

The geometries of the reactants, products, intermediates, and transition states on the potential energy surface (PES) of the title reaction system are found at

* E-mail: wangrs@nenu.edu.cn
Received October 23, 2003; revised January 4, 2004; accepted February 16, 2004.
Project supported by the Natural Science Foundation of Jilin Province (No. 20010344), the Foundation of Education Bureau of Hainan Province (No. hjkj200312), and the Science Foundation for Excellent Youth of Northeast Normal University (No. 111382).

B3LYP/6-311+G** level. These structures are displayed in Figure 1, while their total energies, zero-point energies, single-point energies, and relative energies are listed in Table 1. Furthermore, a schematic potential energy surface (PES) of the title reaction is shown in Figure 2.

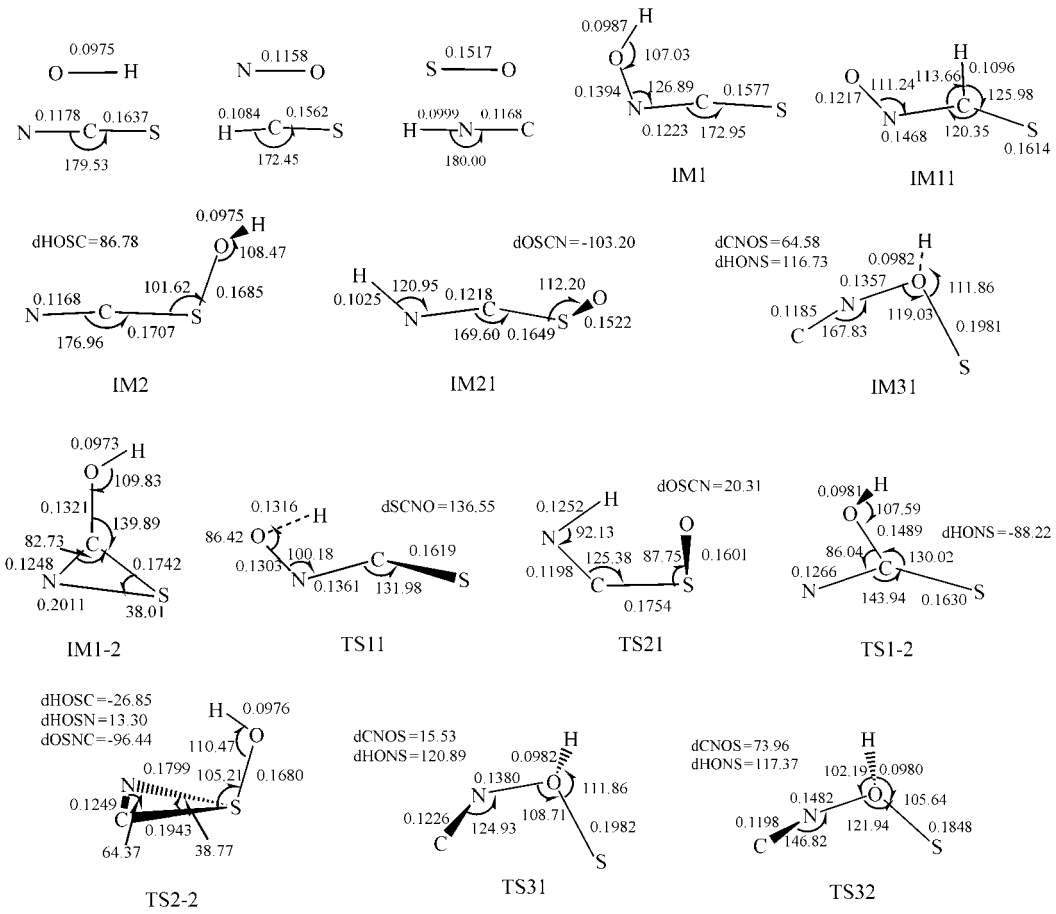

Figure 1 Optimized geometries of reactant, intermediates, transition states and products (bond length unit: nm, angle unit: degree).

Table 1 Total (hartree) and relative (kJ • mol^{-1}) energies of all stationary points on the potential energy surface of NCS and OH radicals reaction

	E_{ZPC}	$E_{(0)B3LYP/6-311+G^{**}}$	$E_{QCISD(T)/6-311+G^{**}}$	E_{rel}
NCS+OH	0.015357	−566.708748	−565.842494	0
IM1	0.023818	−566.765222	−565.916886	−195.317
TS11	0.016603	−566.641409	−565.787362	144.748
IM11	0.022415	−566.733664	−565.897733	−145.031
HCS+NO	0.015085	−566.681362	−565.834747	20.339
IM2	0.022745	−566.791806	−565.958531	−304.656
TS21	0.016873	−566.680334	−565.832655	25.831
IM21	0.022014	−566.750741	−565.903257	−159.534
TS31	0.021793	−566.595772	−565.757307	223.657
IM31	0.021883	−566.607150	−565.768759	193.590
TS32	0.020282	−566.606459	−565.762535	209.931
HNC+SO	0.019947	−566.708970	−565.866386	−62.730
IM1-2	0.023787	−566.767256	−565.934579	−241.770
TS1-2	0.021341	−566.710525	−565.871575	−76.353
TS2-2	0.020368	−566.723800	−565.885213	−112.160

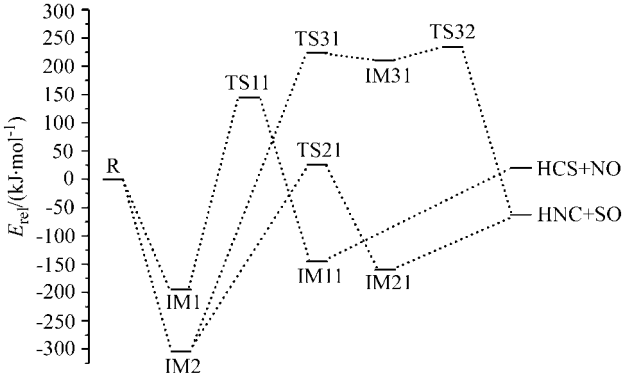

Figure 2 Relative energies (kJ • mol^{-1}) on the potential energy surface of NCS and OH radicals reaction.

Reaction mechanism

The calculation results show that the potential energy surface of the title reaction is complex. Starting from the original reactant R, three possible channels are found on the PES. These reaction channels are as follows:

Path I R→IM1→TS11→IM11→HCS+NO
Path II R→IM2→TS21→IM21→HNC+SO
Path III R→IM2→TS31→IM31→TS32→HNC+SO

We consider two possible initial attack sites of OH at NCS, *i.e.*, O—N attack, and O—S attack, and both sites are competitive. Two attacks can barrierlessly lead to two initial intermediates IM1 (for O—N) and IM2 (O—S), and both are stable intermediates. The sufficient internal energies of IM1 and IM2 are available for subsequent isomerization. There are double isomers for both IM1 and IM2, due to rotating round O—N bond and O—S bond. It is interesting that IM1 and IM2 can convert into each other via various isomers.

For path I, the oxygen atom of OH attacks nitrogen atom in NCS to yield the initial plane IM1, which is 195.317 kJ • mol^{-1} more stable than the reactant, by forming an O—N bond. The O—N distance in IM1 is 0.1394 nm, which is a little longer than the equilibrium value of the O—N single bond length. The reaction proceeds from IM1 through TS11, which is 144.748 kJ • mol^{-1} higher in energy than the reactant, via the breaking of the H—O bond and the formation of the H—C bond, to produce IM11, which is 145.031 kJ • mol^{-1} more stable than the reactant. In this process, the hydrogen atom shifts from the oxygen atom to the carbon atom with the energy barrier being 289.779 kJ • mol^{-1}. The IM11 then undertakes dissociation of C—N bond into HCS+NO, which is 20.339 kJ • mol^{-1} less stable than the reactant.

For path II, the oxygen atom attacks sulfur atom to yield the initial nonplanar IM2, which is 304.656 kJ • mol^{-1} lower than the reactant, by forming an O—S bond. The O—S distance in IM2 is 0.1685 nm, the normal O=S double bond length. Starting from the IM2 the second pathway evolves now through TS21 for the transfer of H from the O atom to the N atom to give IM21. TS21 is 25.831 kJ • mol^{-1} above the reactant and IM21 is 159.534 kJ •mol^{-1} more stable than the reactant. From IM2 to TS21 the hydrogen atom dissociates from the oxygen atom and recombines with the nitrogen atom with the energy barrier of this process being 330.487 kJ • mol^{-1}. The IM21 proceeds dissociation of C—S bond into HNC+SO, which is 62.730 kJ • mol^{-1} more stable than the reactant.

The third pathway proceeds initially from the IM2. The N atom of IM2 closes firstly to O atom forming N—O bond and then the C—S bond stretches and breaks to give TS31, which is 223.657 kJ • mol^{-1} less stable than the reactant with an energy barrier of 528.313 kJ • mol^{-1}. This step is the rate controlling step for path III. The TS31 evolves through IM31 and TS32, which are 193.590 kJ • mol^{-1} and 209.931 kJ • mol^{-1} higher in energy than the reactant, respectively, leading to the product HNC+SO. The OH inserts between the N atom and S atom with the atoms rearranging in molecule because of the high energy barrier, we consider that the third pathway should be difficult to react, and the path I and path II should be the main channels.

Isomerization

The isomerization between IM1 and IM2 starts from the IM1 to the IM1-2 through TS1-2, 76.353 kJ • mol^{-1} more stable than the reactant, during which the OH shifts from N atom to C atom. IM1-2, 241.770 kJ •mol^{-1} under the reactant, has a tricircle structure and proceeds into IM2 with the transposition of OH from C atom to S atom. The reverse process is the isomerization from IM2 to M1. IM1-2 has two isomers for rotating around O—C bond. The isomeric process of the two IM2 isomers evolves through TS2-2, which is 112.160 kJ • mol^{-1} more stable than the reactant and possesses tricircle structure, for the bonding and breaking of N—S bond.

Rate constants

Dual-level dynamics calculations for both path I and path II were carried out with the VTST-ISPE approach at the QCISD(T)/6-311+G**//B3LYP/6-311+G** level. The rate constants were evaluated by TST (conventional transition state theory) and CVT (canonical variational transitional state theory) over a temperature region from 800 to 2500 K. In order to calculate the rate constants, 30 points have been selected near the transition state region along MEP—15 points in the reactant zone and 15 points in the product zone. Figures 3a—3b show the calculated TST and CVT rate constants for both path I and path II, respectively, against the reciprocal of the temperature. It is noted that the rate constants for both path I and path II are negatively dependent on temperature, which are comparable with the reactions of NCS with NO and NO_2.[15] These theoretical kinetic properties for reaction of NCS and OH are similar with the ex-

perimental result for reactions of NCS with NO and NO_2. It can be seen that the TST and CVT rate constants have a large difference over the whole temperature range, showing that the variational effect for the rate constant calculation plays an important role, especially for path I.

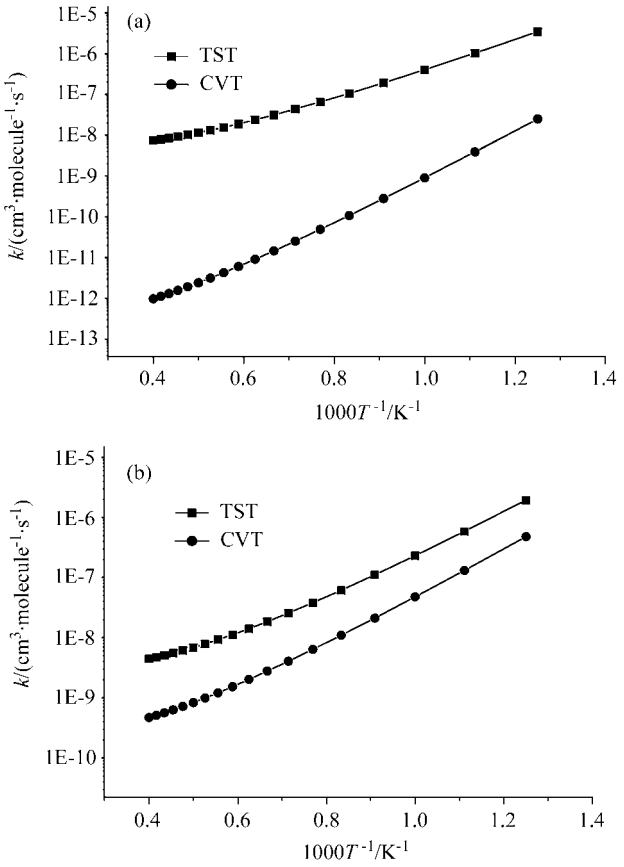

Figure 3 Rate constant for path I (a) and path II (b) as functions of the reciprocal of the temperature (K) over the temperature range of 800—2500 K.

Conclusions

In the present work, a detailed theoretical investigation for the reaction of NCS radical with OH was carried out. The following conclusions can be predicated.

1. The mechanism of the title reaction involves three channels. Path I and path II are the main channels and competitive, with some advantages for path I in kinetics. Because of the high energy barrier, it should be difficult to react for the third pathway.

2. According to the rate constant calculation results, the rate constants of both path I and path II are negatively dependent on temperature, and are comparable with the reactions of NCS with NO and NO_2, and are similar with the experimental result of those reactions. It also can be shown that the variational effect plays an important role in the rate constant calculation over the whole temperature ranges, especially for path I.

References

1 Miller, J. A.; Bowman, C. T. *Prog. Energy Combust. Sci*. **1989**, *15*, 287.
2 Perry, R. A.; Siebers, D. L. *Natrue* **1986**, *324*, 657.
3 Miller, J. A.; Bowman, C. T. *Int. J. Chem. Kinet*. **1991**, *23*, 289.
4 Perry, R. A. *J. Chem. Phys*. **1985**, *82*, 5485.
5 Atakan, B.; Wolfrum, J. *Chem. Phys. Lett.* **1991**, *78*, 157.
6 Juang, D. Y.; Lee, J. S.; Wang, N. S. *Int. J. Chem. Kinet*. **1995**, *27*, 1111.
7 Cooper, W. F.; Hershberger, J. F. *J. Phys. Chem*. **1992**, *96*, 771.
8 Cooper, W. F.; Park, J.; Hershberger, J. F. *J. Phys. Chem*. **1993**, *97*, 3283.
9 Park, J.; Hershberger, J. F. *J. Phys. Chem*. **1993**, *97*, 13647.
10 Park, J.; Hershberger, J. F. *Chem. Phys. Lett*. **1994**, *218*, 537.
11 Campomanes, P.; Menendez, I.; Sordo, T. L. *J. Phys. Chem. A* **2001**, *105*, 229.
12 Liu, P.-J.; Pan, X.-M.; Zhao, M.; Su, Z.-M.; Wang, R.-S. *Acta Chim. Sinica* **2002**, *60*, 1941 (in Chinese).
13 Northrup, F. J.; Sears, T. J. *J. Chem. Phys*. **1990**, *93*, 2337.
14 Ruscic, B.; Berkowitz, J. *J. Chem. Phys*. **1994**, *101*, 7975.
15 Baren, R. E.; Hershberger, J. F. *J. Phys. Chem*. **1999**, *103*, 11340.
16 Frisch, M. J.; Trucks, G. W.; Schlegel, H. B.; Scuseria, G. E.; Robb, M. A.; Cheeseman, J. R.; Zakrzewski, V. G.; Montgomery, J. A.; Stratmann, Jr., R. E.; Burant, J. C.; Dapprich, S.; Millam, J. M.; Daniels, A. D.; Kudin, K. N.; Strain, M. C.; Farkas, O.; Tomasi, J.; Barone, V.; Cossi, M.; Cammi, R.; Mennucci, B.; Pomelli, C.; Adamo, C.; Clifford, S.; Ochterski, J.; Petersson, G. A.; Ayala, P. Y.; Cui, Q.; Morokuma, K.; Malick, D. K.; Rabuck, A. D.; Raghavachari, K.; Foresman, J. B.; Cioslowski, J.; Ortiz, J. V.; Baboul, A. G.; Stefanov, B. B.; Liu, G.; Liashenko, A.; Piskorz, P.; Komaromi, I.; Gomperts, R.; Martin, R. L.; Fox, D. J.; Keith, T.; Al-Laham, M. A.; Peng, C. Y.; Nanayakkara, A.; Challacombe, M.; Gill, P. M. W.; Johnson, B.; Chen, W.; Wong, M. W.; Andres, J. L.; Gonzalez, C.; Head-Gordon, M.; Replogle, E. S.; Pople, J. A., *Gaussian 98*, Revision A.9, Gaussian, Inc., Pittsburgh PA, **1998**.
17 Corchado, J. C.; Chuang, Y.-Y.; Fast, P. L.; Villa, J.; Hu, W.-P.; Liu, Y.-P.; Lynch, G. C.; Nguyen, K. A.; Jackels, C. F.; Melissas, V. S.; Lynch, B. J.; Rossi, I.; Coitino, E. L.; Ramos, A. F.; Pu, J.-Z.; Albu, T. V., Department of Chemistry and Supercomputer Institute, University of Minnesota, Minneapolis, Minnesota; Steckler, R., San Diego Supercomputer Center, La Jolla, California; Garrett, B. C., Environmental Molecular Sciences Laboratory, Pacific Northwest Laboratory, Richland, Washington; Isaacson, A. D., Department of Chemistry, Miami University, Oxford, Ohio; Truhlar, D. G., Department of Chemistry and Supercomputer Institute, University of Minnesota, Minneapolis, Minnesota, *POLYRATE*, Version 9.0, May, **2002**.

(E0310239 CHENG, B.)